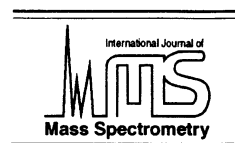




ELSEVIER

International Journal of Mass Spectrometry 210/211 (2001) 101–111



www.elsevier.com/locate/ijms

# Noise analysis for 2D tandem Fourier transform ion cyclotron resonance mass spectrometry

Guillaume van der Rest, Alan G. Marshall\*

*Center for Interdisciplinary Magnetic Resonance, National High Magnetic Field Laboratory, Florida State University,  
1800 East Paul Dirac Drive, Tallahassee, FL 32310, USA*

Received 31 December 2000; accepted 12 February 2001

## Abstract

In principle, two-dimensional (2D) Fourier transform ion cyclotron resonance (FTICR) mass spectrometry offers identification of all precursor-product ion pairs (equivalent to all precursor ion scans, all product ion scans, and all neutral loss scans), as well as relative rate constants for all precursor gas-phase ion–molecule reactions and distinction between fragmentation and adduction processes, in a single, automatically acquired data set. However, although the principles of 2D FTICR techniques were demonstrated more than ten years ago, very few analytical applications have yet been demonstrated. Here, we apply 2D FT/FTICR tandem mass spectrometry, by stored waveform inverse Fourier transform modulation of ion cyclotron radius (and thus ion kinetic energy), to an experimental mixture of proton-bound (and sodium-bound) amino acid dimer ions. Although several ion fragmentation pathways may be identified, interpretation is hindered by significant noise along each slice passing through a precursor ion peak on the diagonal of the 2D mass spectrum. By analogy to “ $t_1$ ” noise in 2D nuclear magnetic resonance spectroscopy, we are able to simulate such noise by varying the absolute and relative numbers of trapped precursor ions in data acquisitions corresponding to different horizontal slices of the final 2D spectrum. Signals at harmonic multiples of the ion cyclotron frequencies are well modeled by simulations allowing for nonlinear dependence of product ion abundance on precursor ion cyclotron radius modulation magnitude. The present results show that successful future implementation of 2D FT/FTICR tandem mass spectrometry experiments will require careful control of the number of trapped precursor ions, to avoid loss in dynamic range by “contamination” of the rest of the mass spectrum by signals from the most abundant ions. (Int J Mass Spectrom 210/211 (2001) 101–111) © 2001 Elsevier Science B.V.

*Keywords:* Fourier transform; Ion cyclotron resonance; ICR; 2D FTICR; FTMS; MS/MS; mixture analysis

## 1. Introduction

One-dimensional “double-resonance” nuclear magnetic resonance (NMR) techniques [1] were re-

placed by multidimensional Fourier transform NMR spectroscopy (FT-NMR) [2] shortly after it became available. Although the two-dimensional (2D) experiment is less efficient (because it requires interrogation at every discrete spectral frequency rather than just at the NMR frequencies of the peaks of interest), it offers the very great advantage that it is automated, both in implementation and in interpretation, thereby greatly expanding number of researchers who can

\*Corresponding author. E-mail: marshall@magnet.fsu.edu Also with: Department of Chemistry, Florida State University, Tallahassee, FL 32306, USA

Dedicated to Professor Nico Nibbering on the occasion of his retirement.

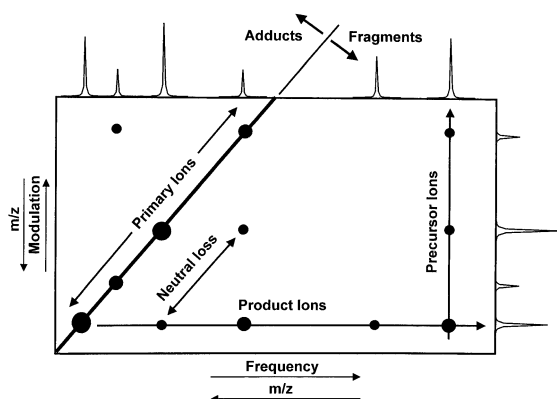


Fig. 1. Schematic 2D FT/FTICR mass spectrum, viewed from above as constant-magnitude contours. Appropriate slices through this single display yield: the precursor ion  $m/z$  spectrum (diagonal slice); an  $m/z$  spectrum of all product ions from a given precursor ion (product “scan,” horizontal slice), an  $m/z$  spectrum of all precursors leading to the same product (precursor scan, vertical slice), and all precursor/product pairs differing by loss of the same neutral (neutral loss scan, slice parallel to diagonal). Adducts and fragments are also readily distinguished, and the relative magnitudes of the off-diagonal peaks correspond to the relative rates for ion–neutral fragmentation or reaction (see text).

exploit the method to determine through-bond (scalar) and through-space (dipolar) couplings between magnetic nuclei in a molecule. In fact, Ernst’s development of 2D NMR contributed at least as much as his development of one-dimensional FT-NMR to his 1991 Nobel Prize recognition.

2D Fourier transform ion cyclotron resonance mass spectrometry (FTICRMS) in principle offers similar advantages for identifying pairs of ions “coupled” by ion–molecule reactions or dissociative collisions, as seen in Fig. 1. As explained in more detail in the following discussions, the precursor ion mass (or cyclotron frequency) spectrum is located on the diagonal of a 2D plot of iso-magnitude contours. Ion products of reaction or dissociation of a given precursor ion appear as peaks along a horizontal slice passing through the precursor ion mass (or cyclotron frequency), to yield a “product ion spectrum.” Similarly, peaks along a vertical slice passing through a given product ion mass (or cyclotron frequency) identify all of the precursors leading to that product, to yield a “precursor ion spectrum.” Peaks along a line parallel to the diagonal identify precursor/product ion

pairs differing by the loss of the same neutral mass, to give a “neutral loss spectrum.” Products with  $m/z$  values lower than that of their precursor (e.g. singly charged fragments of a singly charged precursor) appear to the right of the diagonal, whereas products with  $m/z$  values greater than that of their precursor (e.g. adducts or charge-reduced ions) appear to the left of the diagonal. Finally, the relative magnitudes of the off-diagonal peaks correspond to the relative rates for the ion–neutral collisions or reactions that formed them. Thus, in a single 2D FTICR mass spectrum, one can in principle identify all ion fragmentation/reaction pathways and kinetics, in a single automated experiment.

Three primary methods have been devised to add a second dimension to FTICR mass spectra. The first method is by analogy to 2D nuclear Overhauser enhancement spectroscopy (NOESY [3]); a delay,  $t_1$ , between two excitation events results in modulation of the ion radius depending on the phase of the ion motion at the onset of the second excitation [4,5]. Second, in the stored-waveform ion radius modulation (SWIM) technique [6], the same effect is achieved by replacing the series of incremented temporal delays by a series of stored-waveform inverse Fourier transform (SWIFT) [7,8] excitations. Both of these methods involve Fourier data reduction in both dimensions, and may thus be considered “FT/FT” experiments. A third approach is to encode/de-encode data in the second dimension by Hadamard rather than Fourier transformation [9–11]. Since Fourier transform data reduction is still used for the other dimension, this approach may be denoted “HT/FT.” As with FT/FTICRMS, the HT/FT approach allows recovery of a one-dimensional tandem mass spectrometry (MS/MS) spectrum from a linear combination of spectra containing more than one precursor peak.

Despite its potential major advantages, 2D FT-ICRMS has not yet supplanted one-dimensional MS/MS methods [12,13]. In fact, although the first 2D FT/FTICRMS experiment was described by Bodenhause and co-workers in 1987 [4], only a handful of applications have since appeared, for several reasons, the first of which is well known and the rest of which form the subject of this article. First, mass spectra are

typically much more sparse than NMR spectra. Thus, the competing one-dimensional MS/MS experiment requires one spectrum to isolate each of a relatively small number of precursor ions, whereas the corresponding FT/FT experiment requires acquisition of  $N$  spectra, in which  $N$  is the desired resolving power in the second dimension (say, 256, 512, etc.). Thus, a net gain obtains only if the improvement in signal-to-noise (S/N) ratio compensates for the larger required number of spectra. For example, if a FT/FT mass spectrum requires 256 spectra, and if co-addition of 5 one-dimensional MS/MS spectra suffice to yield an acceptable S/N ratio, then the FT/FT experiment will be preferred only if the number of precursor ions exceeds  $256/5 \approx 51$ . Of course, the FT/FT experiment improves the S/N ratio by a factor of up to  $N^{1/2}$  relative to the one-dimensional MS/MS experiment, but that improvement may not be needed if the initial S/N ratio is sufficiently high. For this reason, the FT/FT experiment is usually not worth considering for samples consisting of relatively few components. [The HT/FT approach avoids this difficulty, but requires a priori knowledge of the precursor ion mass-to-charge ( $m/z$ ) ratios.]

However, recent interest and demonstration of the advantages of FTICRMS for analysis of complex mixtures, ranging from hydrocarbons [14,15] to digests of proteins [16], has revived interest in the 2D approach. The prospect of automated MS/MS analysis of such mixtures could help to discriminate isomers (by fragmentation or ion–molecule reaction), or generate partial amino acid sequences of peptides.

In this article, we apply the SWIM FT/FTMS method to a complex mixture, namely, proton-bound dimers and sodium-bound dimers of amino acids. Facile collision-induced fragmentation of the dimers simplifies the experiment. We originally intended to simplify proton affinity measurements by creating and analyzing the fragmentations of a number of dimers simultaneously. In the course of that effort, we identified a major problem in applying 2D ICRMS to a complex sample with a wide dynamic range of precursor ion relative magnitudes: namely, the high level of  $t_1$  (modulation) noise. Simulations allow us to identify four major sources of such  $t_1$  noise. The first

is “white” noise due to random variation in the number of trapped ions from one data set to the next. This problem is even more severe for electrospray ionization than for previous electron ionization experiments. A second problem is “pink” noise (predominantly at low frequency due to slow variation in the number of trapped ions over the duration of the experiment. A third source of distortion (as well as appearance of signals at unwanted harmonic frequencies) is the nonlinearity of fragmentation efficiency as a function of excitation magnitude. A final source of noise is the small random variation in the relative abundance of trapped ions of different  $m/z$  values.

## 2. Theory

The principles of SWIM excitation for 2D FT/FTICRMS were laid out by Ross et al. in 1993 [6]. A sinusoidal modulation of the cyclotron radius of the ions at each frequency of the precursor ion region is achieved by applying a series of excitation waveforms that are also sinusoidal in the frequency domain. Each time-domain waveform is generated by inverse Fourier transform of the desired frequency-domain magnitude spectrum [17]. The excitation magnitude,  $M_j(\nu)$ , at a given frequency  $\nu$  ( $\nu_{\text{low}} \leq \nu \leq \nu_{\text{high}}$ ) for the  $j$ th modulation waveform ( $0 \leq j \leq n$ ) is given by

$$M_j(\nu) = \frac{1 - \cos\left(j\pi\left(\frac{\nu - \nu_{\text{low}}}{\nu_{\text{high}} - \nu_{\text{low}}}\right)\right)}{2} \quad (1)$$

From Eq. (1), the modulation waveform magnitude spectrum is zero for a precursor ion cyclotron frequency,  $\nu_{\text{low}}$ . The excitation for a precursor ion whose cyclotron frequency falls at the midpoint between  $\nu_{\text{low}}$  and  $\nu_{\text{high}}$  is modulated at magnitudes, (1/2, 1, 1/2, 0, 1/2, 1, . . .), through  $n/4$  cycles. For a precursor ion of the highest cyclotron frequency,  $\nu_{\text{high}}$ , the modulation takes the values (1, 0, 1, 0, . . .), through  $n/2$  cycles. Since the data are decoded by a Fourier transform, this (maximum frequency) modulation matches the Nyquist criterion exactly, so that no aliasing (foldover) occurs. Therefore, to each frequency,  $\nu$ , in

the precursor ion range is associated one unique modulation frequency,  $\nu_{\text{mod}}$ , in the second dimension. The relationship between those frequencies is

$$\nu_{\text{mod}} = \frac{n}{2} \frac{\nu - \nu_{\text{low}}}{\nu_{\text{high}} - \nu_{\text{low}}} \quad (2)$$

In this configuration, the series of ion excitations effectively modulates the cyclotron radius of each precursor ion of different  $m/z$  at a different frequency. Note that Fourier data reduction in the second dimension will be valid only if the product ion relative abundance varies linearly with precursor ion cyclotron radius. In particular, if the ion speed in a plane perpendicular to the applied magnetic field is fast enough that the hard-sphere collision model can be applied (namely, an ion cyclotron radius greater than  $\sim 1$  mm [18]), then the ion–neutral collision frequency is proportional to ion speed and thus to ion cyclotron radius [19].

### 3. Experimental

#### 3.1. FTICRMS experiments

Proline, isoleucine, and phenylalanine were purchased from Sigma (St-Louis, MO) and used without further purification. Solvents (HPLC grade) were purchased from J.T. Baker (Phillipsburg, PA). The various amino acids were dissolved in methanol: water:acetic acid (50:50:2) at a concentration of 100  $\mu\text{M}$  to 1 mM. (A rather high concentration of analyte was needed to generate good abundances of proton-bound dimer ions.)

FTICR mass spectrometry was performed with a passively shielded 9.4 T instrument configured for external accumulation of ions [20] and controlled by a modular ICR data acquisition system (MIDAS) [21]. The microelectrospray ionization [22] flow rate was 0.3 to 0.5  $\mu\text{L}/\text{min}$ , and ions were accumulated in the first octopole for 1–3 s. Adjustment of the octopole frequency to 2.5 MHz partially eliminated lower-mass monomeric ions. The relative concentrations of the three amino acids in the solution were adjusted to

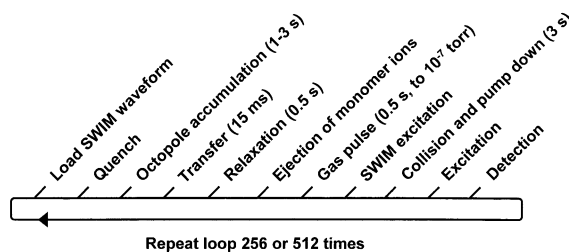


Fig. 2. Experimental event sequence (time axis not to scale) for 2D ESI FT/FTICR mass spectrometry (see text).

yield comparable relative FTICR mass spectral peak magnitudes for the various homo- and heterodimers.

A typical experimental event sequence is shown schematically in Fig. 2. The 256 or 512 SWIM excitation waveforms were generated by an extension of the MIDAS SWIFT generator. The user inputs only the frequency limits ( $\nu_{\text{low}}$  and  $\nu_{\text{high}}$ ), the magnitude limits (see Sec. 4), the desired number of waveforms, and the desired waveform shape. The required number of 32 K waveforms is then generated and stored. The MIDAS control software then loads the waveforms as needed, and records 64 K time-domain transients for 256 or 512 successive cycles. A controlled pulse of argon ( $10^{-7}$  Torr) before the SWIM excitation event provides a collision gas. Ions are then allowed to collide with bath gas during a 3 s pump-down period. Because the actual pressure in the ICR cell is not precisely controlled during the experiment, it is difficult to assess whether single or multiple collision conditions apply.

Two-dimension transformation of the data set was performed by use of a specific extension of the MIDAS software, which allows for various apodization and zero-filling operations to be performed in both dimensions of the dataset. Also, the order of the Fourier transform can be specified: one can either transform each time-domain data (row) to a (one-dimensional) magnitude spectrum and then the transform the modulation domain data (column), or one may FT the modulation domain to yield a (one-dimensional) complex spectrum and then transform the complex time-domain data. The order in which the transforms are applied does not significantly change the resulting spectrum. Stan-

standard Hamming apodization and one zero-filling [23] were performed in both the time and modulation domains.

### 3.2. Simulations

A simulation program takes as input the set of mass-to-charge ratios, whose magnitudes (both total number of ions and relative numbers of ions of different  $m/z$ ) can vary from one excitation modulation to the next. The fragmentation magnitude was set to match the experimental magnitude (namely,  $\sim 20\%$  extent of fragmentation at maximum excitation energy), and a dissociation versus energy curve was set at a defined threshold above which the extent of fragmentation varies linearly with precursor ion kinetic energy. That threshold was set at the same level for every species. (Although we expect different threshold energy for different dimers, the thresholds in this example are close enough so that this assumption does not greatly alter the simulation results. Similarly, we did not attempt to define the relative abundances of the various MS/MS product ions—although calculable from the kinetic method, they are not important for the present demonstration.) From the collision-induced dissociation (CID) product ion relative magnitudes, we generated a reconstructed series of time-domain transients, which were then processed by exactly the same software and with the same data manipulation as the experimental data.

## 4. Results and discussion

### 4.1. Mass spectrum of a multicomponent mixture

Proton affinities may be estimated by producing proton-bound heterodimers in an electrospray ionization (ESI) source and measuring product ion abundance ratios from the MS/MS fragmentation patterns for these dimers, by means of the “kinetic method” developed by Cooks and co-workers [24]. Our original goal was to amplify that approach by producing MS/MS spectra not one at a time, but rather a whole series in a single experiment. Initially, due to lack of

Table 1

Proton affinity (PA) and gaseous basicity (GB), in kJ/mol, for each of the amino acids in the present experiments [26]

Amino acid	PA	GB
Isoleucine	917.4	883.5
Proline	920.5	886.0
Phenylalanine	922.9	888.9

precise control of the fragmentation energy, the goal was to rank proton affinities qualitatively, based on fragment ion relative magnitudes. Our experiment thus resembles multiple simultaneous bracketing [25] rather than a true proton affinity measurement. We then intended to proceed, by modeling the energetic conditions as a function of the modulation magnitude, to a complete analysis based on the kinetic method. A simple mixture of three amino acids (Pro, Ile, and Phe) was chosen as a test case, because their tabulated proton affinities are similar (Table 1), so that strong proton-bound heterodimer formation is predicted. The concentration ratios of the three amino acids were adjusted (Ile/Phe/Pro, 3/2/1) so as to produce comparable relative abundances of the various heterodimers (see Fig. 3). Although only three individual compounds are present in solution, the high concentration of amino acids led to the formation of a number of gas-phase adduct ions: the six expected proton-bound homo- and heterodimers, six lower-abundance sodi-

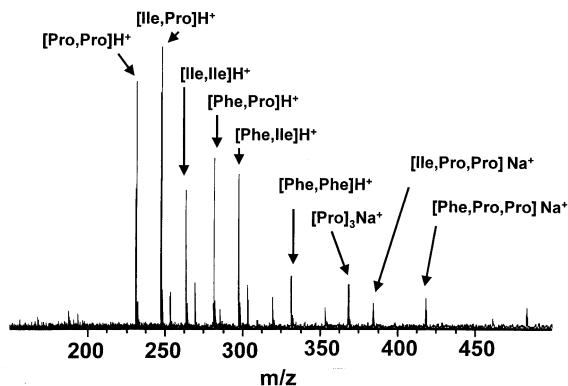


Fig. 3. ESI FTICR mass spectrum of a (3:2:1) isoleucine:phenylalanine:proline amino acid mixture, at a total concentration of 1 mM. The low-magnitude unlabeled peaks between the proton-bound dimers are the corresponding sodium-bound dimers.

um-bound dimers, and even some sodium-bound trimers ( $[\text{Pro}]_3\text{Na}^+$ ,  $[\text{Ile,Pro,Pro}]\text{Na}^+$ ,  $[\text{Phe,Pro,Pro}]\text{Na}^+$ ) could be identified. The presence of these additional sodiated species adds to the complexity of the spectrum, and enhances its value for resolving multiple precursor/product pairs in the 2D experiment.

#### 4.2. Experimental 2D mass spectrum

Our first FT/FTICR mass spectra exhibited a very strong contamination in the modulation dimension by relatively high-magnitude peaks at multiple harmonics of the expected ion cyclotron frequency. The presence of harmonic signals indicates that excitation of the precursor ions occurs over a range of cyclotron radius within which ion fragmentation does not vary linearly with precursor ion radius. The nonlinearity arises in two primary ways. First, linearity obtains only above a minimum precursor ion kinetic energy—at lower precursor energy, the product ion spectra (horizontal slices in Fig. 1) are distorted. Conversely, at sufficiently high radius modulation amplitude, precursor ions are ejected radially before they can fragment—that effect primarily distorts the precursor ion spectra (vertical slices in Fig. 1).

This problem was anticipated [6], and the solution is to modulate between a nonzero initial radius and a maximum radius at which precursor ions are not ejected in significant number. Experimentally, broadband SWIFT excitation of the ions was adjusted to yield minimum excitation at an amplitude at which product ion abundance reached  $\sim 5\%$  of the initial precursor ion population. Maximum excitation amplitude was chosen at  $\sim 5$  times the lowest excitation energy. Thus, a typical SWIM excitation waveform defines a sinusoid varying between 20% and 100% of maximum magnitude (Fig. 4). The frequency boundaries are chosen to span only the frequencies of the precursor ions of interest (from 700 kHz/206.1 Da to 400 kHz/360.6 Da), because there is no need to modulate the radius of ions not present in the precursor  $m/z$  spectrum.

A typical resulting ESI FT/FTICR mass spectrum is shown in Fig. 5. As in Fig. 1, the  $m/z$  spectrum of

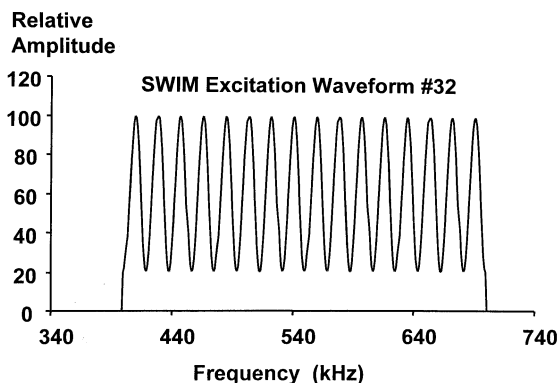


Fig. 4. Ion modulation stored waveform no. 32 of a sequence of 256 excitation wave forms of a 2D FTICR experiment. The minimum magnitude is set at 20% of the maximum magnitude, so that ion kinetic energy always exceeds the threshold above which fragmentation varies quasilinearly with excitation magnitude (see text).

initially present precursor ions appears on the diagonal (dashed) line extending from lower left (400 kHz, or  $m/z$  360.6) to upper center (700 kHz, or  $m/z$  206.1). Each horizontal slice extending from one of the peaks on the diagonal represents an MS/MS (one-dimensional) spectrum, in which fragment product ions appear at lower  $m/z$  than their precursor ion. (Adduct ions or product ions of lower charge than their precursor ion could appear at higher  $m/z$  (i.e. to the left of the diagonal precursor peak) on the same horizontal slice.) Precursor ions leading to the same product ion appear as peaks on a vertical slice extending downward from where a given product ion would be projected to appear on the diagonal.

As in 2D FT-NMR, it is simpler (with respect to both interpretation and volume of data to be analyzed) to consider one-dimensional slices of the 2D spectrum, to yield one-dimensional equivalent product ion and precursor ion spectra. Before analyzing the fragmentation patterns, we stop to note the presence of numerous above-threshold noise spikes distributed throughout a vertical slice passing through each precursor peak on the diagonal. (Much lower-magnitude noise is similarly distributed along a vertical slice passing through each product ion  $m/z$  as well.) In fact, the magnitude of these precursor-associated noise peaks often exceeds that of the desired off-diagonal product ion signals. The problem

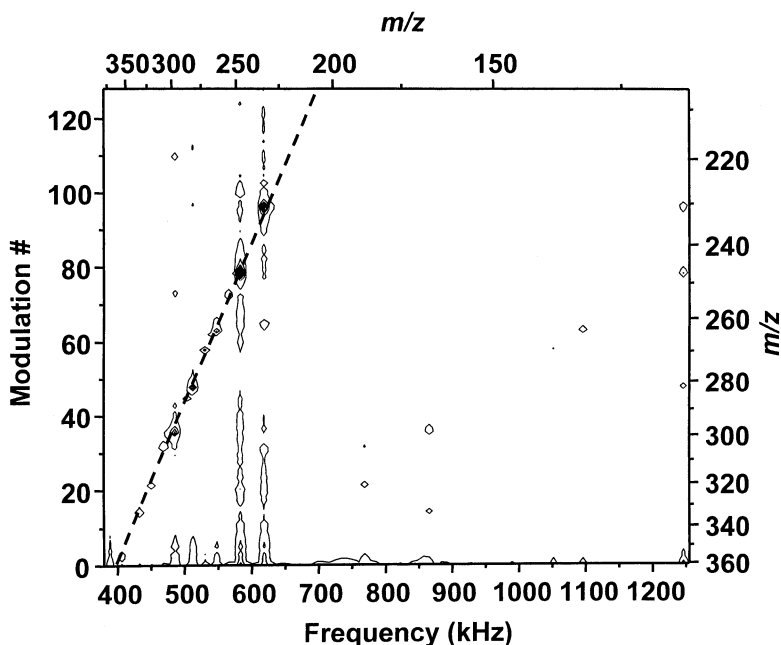


Fig. 5. Constant-magnitude contours of a 2D FT/FTICR mass spectrum, for a mixture of proton-bound dimers and sodium-bound dimers of three amino acids. The top and right axes show the mass-to-charge ratio corresponding to ion cyclotron frequency (bottom) and modulation frequency (left). Starting at a given precursor ion  $m/z$  value on the diagonal (dashed line), a horizontal projection shows a peak at the  $m/z$  of each product ion from that precursor. Conversely, starting at a given product ion  $m/z$  value, a vertical projection shows a peak at the  $m/z$  of each precursor ion leading to that product.

becomes especially evident from comparison of the noise levels (plotted on the same ordinate scale) for horizontal (Fig. 6, left) and vertical (Fig. 6, right) slices through the (Pro,Ile) $H^+$  dimer diagonal peak of

Fig. 5. The noise level in the second dimension (Fig. 6, right) can be as large as  $\sim 20$  times that for the first dimension (Fig. 6, left), when the frequency of a slice passes through an ion cyclotron resonance frequency.

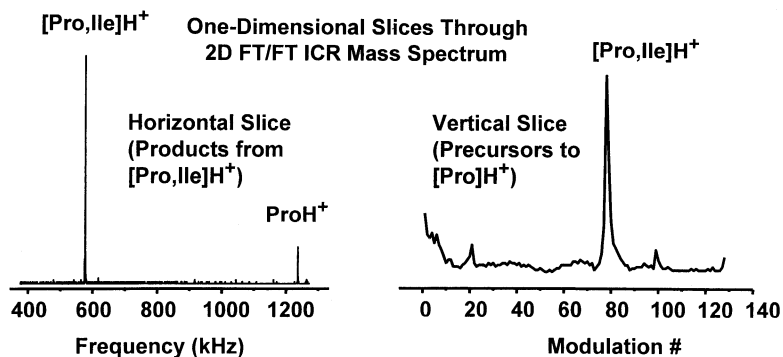


Fig. 6. One-dimensional slices of the 2D FTICR spectrum of Fig. 5. Left: Horizontal slice at modulation no. 79 ([Pro,Ile] $H^+$  precursor ion). This slice may be read as a one-dimensional MS/MS product ion spectrum, in which [Pro,Ile] $H^+$  precursor ions are seen to dissociate to yield [Pro] $H^+$  product ions. Right: Vertical slice (displayed at the same vertical scale) through  $m/z$  247.1 (Ile,Pro) $H^+$ , showing the much higher noise level due to fluctuation in number of precursor ions (" $t_1$ " noise-see text). The small peaks at modulation nos. 100 and 20 correspond to first and second harmonic multiples of the ICR frequency of [Pro,Ile] $H^+$  (see text).

Table 2

Observed fragmentations of the proton-bound dimers and some sodium-bound dimers of three amino acids (Pro, Ile, and Phe); M: high magnitude fragment; m: low magnitude fragment above modulation noise level; ?: magnitude too small to distinguish from noise in the modulation dimension

Dimer	ProH <sup>+</sup>	IleH <sup>+</sup>	PheH <sup>+</sup>	ProNa <sup>+</sup>	PheNa <sup>+</sup>
[Pro,Pro]H <sup>+</sup>	M				
[Pro,Ile]H <sup>+</sup>	M	?			
[Ile,Ile]H <sup>+</sup>		M			
[Pro,Phe]H <sup>+</sup>	M		m		
[Ile,Phe]H <sup>+</sup>		?	M		
[Phe,Phe]H <sup>+</sup>			M		
[Ile,Pro]Na <sup>+</sup>				m	
[Phe,Pro]Na <sup>+</sup>					m
[Phe,Ile]Na <sup>+</sup>					M

In other words, part of the signal magnitude for ions of a given  $m/z$  appears in Fig. 5 as noise distributed along a slice passing through that ion's cyclotron frequency. Finally, although the noise level in a given horizontal slice of Fig. 5 (as in Fig. 6, left) is comparable to that for 10 summed conventional one-dimensional CID MS/MS spectra, close examination reveals that a small (but measurable) noise peak appears at the  $m/z$  of each of the precursor ions (not just the one leading to the product ions on that horizontal slice). Such noise peaks can be especially troublesome if the precursor ion magnitudes vary widely. In the present experiments, we adjusted the amino acid initial concentrations so as to yield dimer ions of comparable relative magnitudes. If, instead, an equimolar mixture of amino acids is used, then the proline and phenylalanine dimer ions dominate the FT/FT spectrum, and even in the horizontal slice for [Ile,Ile]H<sup>+</sup> dimer fragmentation, the dominant peaks are those of [Phe,Pro]H<sup>+</sup> and ProH<sup>+</sup>.

The fragmentation patterns for the six proton-bound dimer ions, inferred from the presence of off-diagonal peaks in the FT/FT spectrum of Fig. 5, are summarized in Table 2. The observed fragmentation behavior deviates somewhat from that based on the proton affinities and gaseous basicities tabulated by Hunter and Lias [26]. However, given that the precise energetic conditions in the 2D experiment are not known (since the cyclotron radius and thus the kinetic energy vary for each experiment, and since

single and multiple collisions may both occur), only qualitative conclusions may be drawn. For the kinetic method [24] to yield an accurate value, a constant effective temperature (or constant collision energy) would be required. Nevertheless, in the absence of major entropic factors, the most abundant product ion would be expected to be the one with the highest proton affinity. The FT/FTICR experiment thus predicts an expected amino acid proton affinity rank order, PA(proline) > PA(phenylalanine) > PA(isoleucine), whereas the NIST tabulation (Table 1) permutes the first two: PA(phenylalanine) > PA(proline) > PA(isoleucine). In support of the present finding, many authors have ranked proline as having a higher proton affinity than phenylalanine, based on the kinetic method [27–29], on bracketing experiments [30], and on high-pressure mass spectrometry equilibrium measurements [31]. Although the present experiment does not definitively resolve the issue, it shows that 2D FT/FTICRMS does have potential value for such measurements, by simultaneously bracketing the proton affinities of a series of compounds with an appropriate (other) series of reference compounds of known proton affinities.

Another interesting feature of this 2D FTICR spectrum is the presence of fragmentation products of three of the sodium-bound dimers (Table 2). With these fragmentary results, we suggest the following ordering of the corresponding sodium ion affinities (SIA): SIA(phenylalanine) > SIA(proline) > SIA(isoleucine), namely, the same order as that given by experiments based on the kinetic method [32].

#### 4.3. Simulated 2D spectra

The results of the previous section demonstrate that 2D FTICR holds significant promise for the characterization of complex mixtures, provided that the level of modulation (second-dimension) noise can be reduced. Fig. 6(right) illustrates several contributions to that noise. First, some harmonic spikes are still visible, although they persist at only ~2 times the noise level. We attribute the harmonic signals to some residual precursor ion ejection and to the nonlinearity of the fragmentation versus precursor ion cyclotron



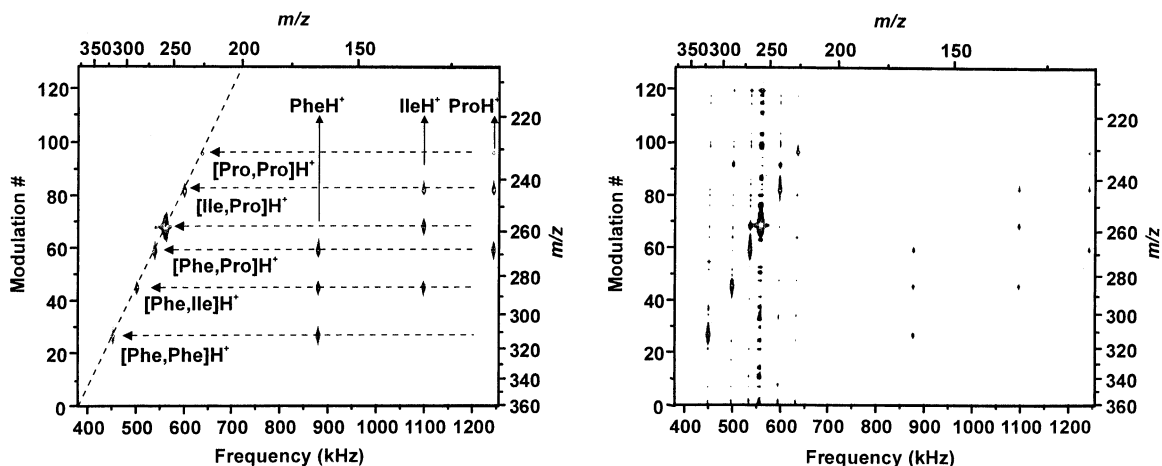


Fig. 7. Simulated 2D FTICR spectra, assuming the same extent of fragmentation for all possible product ions. Left: Ideal behavior (linear system, no noise). The product ion slices (horizontal dashed lines) are shown for each of six precursor ions (except for [Ile,Ile]H<sup>+</sup>, due to lack of space between the lines). The precursors for each of three product ions are shown in the vertical dashed lines. Right: Same data, but with additional 20% random scan to scan fluctuation in total ion population, 10% ejection of precursor ions at high modulation magnitude, 5% slow monotonic variation in the total ion population, and 5% random relative ion population.

radius modulation magnitude at high modulation magnitudes. In any case, the harmonic signals are well localized and do not significantly interfere with data interpretation. Second, the increased noise at low modulation frequency likely arises from slow variation in experimental conditions as the different spectra are sequentially recorded. One could redistribute this noise throughout the entire spectrum by pseudo-random ordering of the modulation wave forms (somewhat like random slice ordering in magnetic resonance imaging data acquisition), but it is as easy to increase slightly the modulation window so that no precursor ions are present in the first modulation cycles. Third, as discussed above, the primary concern is the noise distributed throughout the modulation frequency range, because it can overwhelm the desired signal from products of other precursor ions. This third effect was noted in the first HT/FT experiments [10] where it was denoted as “cross-talk,” and was attributed to variations in ion magnitude from one sequence to the next, for ions generated inside the trap by electron ionization. Variation in number of ions from one spectrum to the next is expected to vary even more for electrospray ionization (as in the present experiments), due to slight changes in the

solution flow rate, drying air current, and any of numerous other parameters. In fact, we observed a 20% variation in the total number of the trapped ions (based on total observed ICR signal) from one spectrum to the next.

Fig. 7(left) shows a 2D FT/FTICR mass spectrum, simulated in the absence of noise or nonlinearity in product ion abundance versus precursor ion cyclotron radius modulation magnitude. Based on the locations of the nine off-diagonal peaks, nine product ions are clearly identified. Horizontal slices passing through diagonal peaks identify the product fragment ions from each of five precursor proton-bound dimer precursor ions. Vertical slices identify the precursor ions whose fragmentation leads to each of three product ions. (Sodium-bound dimers were not included in this simulation.)

Fig. 7(right) shows a simulated FT/FTICR mass spectrum modified to match the experimental 2D spectrum of Fig. 5. The simulation incorporates four sources of modulation noise: a 20% random variation in total ion population from one experiment to the next (based on the experimentally observed variation noted in the preceding paragraph), truncation of 10% of the precursor ion population due to assumed radial

ejection at high modulation amplitude, a slow (5% monotonic increase from modulation no. 1 to modulation no. 256) in mean ion population over the course of the 2D data acquisition period, and a 5% random variation in relative ion abundances from one spectrum to the next. The close agreement between experimental and simulated 2D mass spectra suggests that we have accounted for all of the principal sources of modulation noise in the FT/FTICRMS experiment.

## 5. Conclusions

The present results show that the most important step in making 2D FTICR analytically useful for tandem mass spectrometry analysis of complex mixtures is to reduce the noise in the second (vertical) dimension to an acceptable level. The principal source of that noise is variation in the number of trapped ions from one data acquisition to the next. If one had an independent means of counting the ions, one could (as suggested by Williams et al. for HT/FTICR [10]) scale the magnitude of each time-domain transient signal to account for the varying number of ions. For example, an ion whose  $m/z$  lies outside the modulation excitation range could serve as a reference. The problem, however, is to find a compound that does not react with the mixture, and lies outside the mass range of interest. Another solution could be to sum several time-domain transients for each modulation excitation. However, FT/FTICR experiments already require at least 256–512 separate modulation excitations. The advantage over a standard one-dimensional MS/MS experiment would be lost if too many transients must be required. It is worth noting that our attempts to perform Hadamard transform FTICR spectra of derivatized trypsin digests [33] have hit this same problem of variation in the total amount of ions. Thus, some innovative way of controlling the number of trapped ions produced by an unstable external ESI source will be needed before 2D FTICR can become a widespread analysis tool for MS/MS of complex mixtures.

A second major problem (although not in this example) is that it is difficult in practice to choose a

single range of ICR radius modulation amplitude (FT/FT) or threshold CID energy or infrared irradiation intensity (HT/FT) that applies to all components of a complex mixture [33]. Thus, unless all of the components of the mixture happen to fragment over approximately the same range of collision energy (or multiphoton infrared intensity:duration product), then nonlinearity in the modulation dimension again leads to harmonics and/or absence of off-diagonal peaks due to subthreshold modulation excitation.

In spite of these problems, 2D FT/FTICRMS has proved quite efficient for analysis of the present sample mixture of three electrosprayed amino acids: not only were we able to identify six proton-bound dimers from off-diagonal peaks in the 2D spectrum, but we characterized the dissociation products of three additional sodium-bound dimers, even though experimental conditions had not been optimized for either their production or for their fragmentation. Thus, out of the 12 precursor ions between  $220 < m/z < 360$ , 9 gave rise to interpretable fragmentations when submitted to SWIM experiments. Considering that the three missing fragmentations are those from ions of low initial relative abundance, the 2D method can be deemed successful. Additional experiments conducted by application of HT/FTICR on derivatized tryptic peptide digest mixtures have shown a similar capability of multidimensional techniques in FTICR to perform efficient MS/MS experiments [33].

## Acknowledgements

The authors acknowledge Michael Freitas for initial integration of SWIM into the MIDAS SWIFT generator, and also Fei He and Christopher L. Hendrickson for helpful discussions. This work was supported by the NSF National High Field FT-ICR Facility (CHE-99-09502), Florida State University, and the National High Magnetic Field Laboratory.

## References

- [1] J.D. Baldeschwieler, E.W. Randall, *Chem. Rev.* 63 (1963) 81.
- [2] R.R. Ernst, G. Bodenhausen, A. Wokaun, *Principles of*

- Nuclear Magnetic Resonance in One and Two Dimensions, Oxford University Press, London, 1987.
- [3] G. Bodenhausen, R.R. Ernst, *J. Am. Chem. Soc.* 104 (1982) 1304.
- [4] P. Pfändler, G. Bodenhausen, J. Rapin, R. Houriet, T. Gäumann, *Chem. Phys. Lett.* 138 (1987) 195.
- [5] P. Pfändler, G. Bodenhausen, J. Rapin, M.-E. Walser, T. Gäumann, *J. Am. Chem. Soc.* 110 (1988) 5625.
- [6] C.W. Ross III, S. Guan, P.B. Grosshans, T.L. Ricca, A.G. Marshall, *J. Am. Chem. Soc.* 115 (1993) 7854.
- [7] A.G. Marshall, T.-C.L. Wang, T.L. Ricca, *J. Am. Chem. Soc.* 107 (1985) 7893.
- [8] S. Guan, A.G. Marshall, *Int. J. Mass Spectrom. Ion Processes* 157/158 (1996) 5.
- [9] F.W. McLafferty, D.B. Stauffer, S.Y. Loh, E.R. Williams, *Anal. Chem.* 59 (1987) 2212.
- [10] E.R. Williams, S.Y. Loh, F.W. McLafferty, R.B. Cody, *Anal. Chem.* 62 (1990) 698.
- [11] S. Haebel, T. Gäumann, *Int. J. Mass Spectrom. Ion Processes* 144 (1995) 139.
- [12] *Tandem Mass Spectrometry*, F.W. McLafferty, Wiley, New York, 1983.
- [13] F.W. McLafferty, I.J. Amster, J.J.P. Furlong, J.A. Loo, B.H. Wang, E.R. Williams, in *Fourier Transform Mass Spectrometry: Evolution, Innovation, and Applications*, M.V. Buchanan (Ed.), American Chemical Society Symposium Series Vol. 359, American Chemical Society, Washington, D.C., 1987, pp. 116–126.
- [14] R.P. Rodgers, E.N. Blumer, M.A. Freitas, A.G. Marshall, *Environ. Sci. Technol.* 34 (2000) 1671.
- [15] K. Qian, R.P. Rodgers, C.L. Hendrickson, M.R. Emmett, A.G. Marshall, *Energy Fuels*, 15 (2000) 492.
- [16] D.M. Horn, R.A. Zubarev, F.W. McLafferty, *J. Am. Soc. Mass Spectrom.* 11 (2000) 320.
- [17] L. Chen, A.G. Marshall, *Int. J. Mass Spectrom. Ion Processes* 79 (1987) 115.
- [18] S. Guan, G.-Z. Li, A.G. Marshall, *Int. J. Mass Spectrom. Ion Processes* 167/168 (1998) 185.
- [19] S. Guan, P.R. Jones, *J. Chem. Phys.* 91 (1989) 5291.
- [20] M.W. Senko, C.L. Hendrickson, M.R. Emmett, S.D.-H. Shi, A.G. Marshall, *J. Am. Soc. Mass Spectrom.* 8 (1997) 970.
- [21] M.W. Senko, J.D. Canterbury, S. Guan, A.G. Marshall, *Rapid Commun. Mass Spectrom.* 10 (1996) 1839.
- [22] M.R. Emmett, R.M. Caprioli, *J. Am. Soc. Mass Spectrom.* 5 (1994) 605.
- [23] A.G. Marshall, F.R. Verdun, *Fourier Transforms in NMR, Optical, and Mass Spectrometry: A User's Handbook*, Elsevier, Amsterdam, 1990.
- [24] R.G. Cooks, J.S. Patrick, T. Kothiaho, S.A. McLuckey, *Mass Spectrom. Rev.* 13 (1994) 287.
- [25] G.S. Gorman, I.J. Amster, *Org. Mass Spectrom.* 28 (1993) 1602.
- [26] E.P. Hunter, S.G. Lias, *J. Phys. Chem. Ref. Data* 27 (1998) 413.
- [27] Z. Wu, C. Fenselau, *Rapid Comm. Mass Spectrom.* 6 (1992) 403.
- [28] K. Isa, T. Omote, M. Amaya, *Org. Mass Spectrom.* 25 (1990) 620.
- [29] G. Bojesen, *J. Am. Chem. Soc.* 109 (1987) 5557.
- [30] G.S. Gorman, J.P. Speir, C.A. Turner, I.J. Amster, *J. Am. Chem. Soc.* 114 (1992) 3986.
- [31] M. Meot-Ner, E.P. Hunter, F.H. Field, *J. Am. Chem. Soc.* 101 (1979) 686.
- [32] G. Bojesen, T. Breindahl, U.N. Andersen, *Org. Mass Spectrom.* 28 (1993) 1448.
- [33] G. van der Rest, F. He, A.G. Marshall, S. Hubbard, S. Gaskell, *Proceedings of the 48th ASMS Conference on Mass Spectrometry and Allied Topics*, Long Beach, CA, 2000, Abstract WP225.